The modified two stream instability at nonmagnetic planets.

R. Bingham,[†] V.D. Shapiro,[‡] K.B. Quest,[*] D. Üçer,[‡] and B.J. Kellett,[†]

January 29, 2014

[†]Rutherford Appleton Laboratory, Chilton,Oxon,OX11 0QX, UK, [‡]Department of Physics, University of California, San Diego, La Jolla, CA 92091, *ECE Department, University of California, San Diego, La Jolla, CA 92091,

Abstract

We describe the role the modified two stream instability plays in the interaction of the solar wind with non-magnetized planets. The instability leads to the production of energetic electrons that can be responsible for the observed x-ray emission.

At planets without intrinsic or very weak magnetic fields (Venus, Mars) an ionosphere is the only, however weak, obstacle to the solar wind flow, and the planetary bow shocks are located quite close to the planet. The ionospheres of both Venus and Mars are therefore directly exposed to the solar wind. Data from particle and wave experiments on board Pioneer-Venus Orbiter (PVO) and Phobos-2 spacecrafts revealed the presence of a thin $\Delta \sim 100km$ turbulent transitional layer at the boundary of both ionospheres usually referred as the plasma mantle (Taylor *et al.*, 1980). In the mantle two types of plasmas – solar wind and the ionospheric plasma are present with comparable densities $n \sim 10^2 cm^{-3}$, but however with very different temperatures. The solar wind proton (electron) temperature is equal to $100(30)eV$, and the solar wind drift velocity is close to the proton thermal velocity. For the planetary plasma with oxygen the main ionic species, the oxygen and electron temperatures are close to 1 eV. There is also experimental evidence for the presence of suprathermal electrons with energies exceeding 100 eV (Shutte *et al.*, 1989; Szego *et al.*, 1997) and oxygen (Taylor *et al.*, 1980) populations in the mantle of both Mars and Venus. Finally, the large tailward escape of the planetary ions, most

probably originating from the dayside mantle, has been observed at Mars (Rosenbauer *et al.*, 1989). Since the mantle thickness is much less than the gyroradius of the picked up planetary ion, the usual scheme of $\mathbf{E} \times \mathbf{B}$ pick up of the planetary ions by the solar wind flow is not applicable. Ion pickup of a collective nature organized by waves must be responsible for the observed tailward planetary ion escape. This has been proposed first for Mars (Sagdeev *et al.*, 1990) and then for Venus (Szego *et al.*, 1991). Intense wave activity at the dayside Venusian mantle was observed by the $100Hz$ channel of the PVO electric field detector with amplitudes of the order of around tens of mV/m (Scarf *et al.*, 1980), and even stronger wave activity in the $5 - 50Hz$ frequency range has been observed by the Phobos-2 spacecraft at the boundary of the Martian ionosphere (Grard *et al.*, 1989), both these wave frequency ranges contain the lower-hybrid resonance frequency.

There are two types of instabilities that can be responsible for the observed wave activity at the planets, the modified two stream instability MTSI (McBride *et al.*, 1972; Sagdeev *et al.*, 1990; Shapiro *et al.*, 1995a) and current driven ion acoustic instability (Huba, 1993). Characteristics of the waves excited by these two instability mechanisms are quite different. The MTSI results in the excitation of sufficiently long wavelength oscillations with wavelength of the order of the solar wind electron gyroradius and with frequency close to the lower-hybrid frequency ($30 - 40Hz$ for the mantle conditions). At the same time waves excited by the ion acoustic instability have much shorter wavelengths of the order of electron Debye scale lengths and frequencies close to the ion plasma frequency ($\sim 1kHz$ for the mantle conditions). It was proposed by Crawford *et al.* (1993) that background noise due to the rapid variations of the plasma parameters at the ionospheric boundary, especially of Debye length may be generated contributing to the $100Hz$ signal. At the same time the averaging procedure used in (Shapiro *et al.*, 1995a) for the wave data of approximately 50 orbits demonstrated that the $100Hz$ signal is dominant and real. Finally, a full statistical analysis of the peak values of the wave data performed recently by (Strangeway and Russell, 1996) demonstrated that the $100Hz$ signals are real and well correlated with ionopause crossings. It is generally believed now that the peak at $100Hz$ (unfortunately, measurements at the lower frequency have not been available at PVO) is not excluded from being natural. Therefore, the experimental data demonstrate that the mantle turbulence is dominated by lower-hybrid waves, and a theoretical model explaining this is needed. We proposed such a model based on the modified two stream instability (MTSI). The model is also applicable to the study of the solar wind with artificial releases of plasma, such as in the AMPTE experiments (Bingham *et al.*, 1991).

Analysis of the dispersion relation of MTSI in a 4 component plasma (2 ion and 2 electron components, corresponding to the solar wind and the ionospheric plasmas) has been performed in (Shapiro *et al.*, 1995a). It was concluded that two branches are unstable.

In the vicinity of the lower-hybrid frequency there is a fluid-type branch corresponding to the waves propagating almost transverse to the magnetic field. At the same time the wave data above the lower-hybrid frequency may be attributed to the kinetic branch of the MTSI, corresponding to waves propagating obliquely to the magnetic field and having frequencies several times above the lower-hybrid frequency. A new branch of the MTSI better matching the observational data has been proposed (Dobe *et al.*, 1999). This branch is generated by the interaction between the ionospheric oxygen ions and the cold electron beam created by $\mathbf{E} \times \mathbf{B}$ solar wind pick up.

Electron pick up takes place during several electron gyroperiods, a time interval much shorter than the lower-hybrid wave period. Although the cold electron beam has little kinetic energy of its own, the resonance between the beam and waves can be sustained for a longer time due to electron pick up by the solar wind under the combined action of the magnetic and the convective electric field in the solar wind. This makes it possible to transfer a substantial amount of the energy from the proton flow to the waves. The excited waves are predominantly electrostatic $\omega_{pe} \ll kc$. They propagate over a range of angles $\theta \sim 60 - 90^o$ with respect to the ambient magnetic field.

The dispersion relation describing wave excitation can be written as

$$\frac{\omega_{pe}^2}{\omega_{ce}^2}\left(1+\frac{\omega_{pe}^2}{k^2c^2}\right)-\frac{\omega_{pe}^2}{\left(\omega-ku_e\right)^2}\frac{k_\parallel^2c^2}{k^2c^2+\omega_{pe}^2}+$$

$$\frac{1+w_pZ\left(w_p\right)}{k^2D_p^2}+\frac{1+Z\left(w_i\right)}{k^2D_i^2}=0 \qquad (1)$$

A similar dispersion relation for a two component plasma (the proton flow through electrons) has been derived by (Hsia, 1979) in the hydrodynamical approximation, the kinetic effects have been taken into account by (McBride and Ott, 1972). In Eq.(1) we made the same assumptions as in the numerical simulations described below only one component of the cold fluid electrons is present, both protons and planetary ions are treated kinetically. The following notation is used

$$w_p=\frac{\omega-ku_p}{kv_{Tp}}, \qquad w_i=\frac{\omega}{kv_{Ti}},$$

and $Z(z)=\int_{-\infty}^{\infty}d\xi\frac{e^{-\xi^2}}{z-\xi}$ is the plasma dispersion function. The notation $v_{Tp}\left(v_{Ti}\right)$ for thermal velocities of the protons (ions) and u_e, u_p for the drift velocities of electrons and protons are used. It is assumed that the wave frequency satisfies conditions $\omega_{cp} \ll \omega \ll \omega_{ce}$, correspondingly electrons are magnetized in these oscillations, while protons and ions are not.

The most unstable mode in the solution of the dispersion relation (1) corresponds to the case when the Doppler shifted wave frequency ($\omega - ku_e$) coincides with the frequency of the plasmas eigenmode, in our case the whistler wave. The instability is similar to the well known Buneman instability (Buneman, 1959) of the unmagnetized plasma, when the Doppler shifted wave frequency coincides with the Langmuir frequency. As for the Buneman instability, $\omega \ll ku$, the resonance condition can be written as

$$ku_e = \omega_{ce}\frac{k_{\|}kc^2}{k^2c^2 + \omega_{pe}^2} \tag{2}$$

The numerical solution of the dispersion relation is plotted in Fig. 1. The growth rate of the most unstable mode, satisfying condition (2) is shown as a function of the mode frequency. A parameter which changes along the curve is $\kappa = \frac{k_{\|}}{k}\sqrt{\frac{m_p}{m_e}}$, *i.e.* the angle of wave propagation with respect to the ambient magnetic field. For $\kappa > 1$ the frequency increases almost linearly with κ, while the growth rate reaches its maximum at $\kappa = 6$ and then slowly decreases with κ. Triangles in Figure 1 show the values of the frequency and the growth rate of the most unstable mode obtained in the numerical simulations of (Dobe *et al.*, 1999) for the different values of κ listed in the figure. As can be seen analytical and numerical results are in a good agreement. Simulations of the MTSI have been carried out by Quest *et al.* (1997) and Dobe *et al.* (1999) using a hybrid code with kinetic ions and finite mass electrons. These simulations follow the nonlinear development of the MTSI within the mantle. The linear and nonlinear stages of evolution of this branch of the MTSI has been investigated using the hybrid particle simulation code (Quest *et al.*, 1997). The code treats two ion species (protons and oxygen ions) using particle in cell methods, the electrons are modelled as a fluid, in which inertial and electromagnetic effects are retained. It conserves the total energy and momentum with an accuracy better than one percent. In the simulations of Dobe *et al.* (1999) waves are permitted to propagate at an arbitrary angle with respect to the magnetic field with the boundary conditions (periodic in x) and initialisation (a relative drift between Maxwellian protons and ions) the same as in Quest *et al.* (1997). The parameters used in the simulations are the following: the solar wind is initialized with the drift velocity $u_p = 1.2v_{Tp}$ in the x direction, $v_{Tp} = \sqrt{\frac{T_p}{m_p}}$ is the thermal velocity. The density of protons and oxygen ions are assumed to be equal, and the β for the different plasma components are $\beta_p = 0.8, \beta_i = 0.0032$ and $\beta_e = 0.016$, where β_j is the ratio of plasma thermal pressure to the magnetic pressure for the jth component. If we assume that electron number density is $10^2 cm^{-3}$, then the simulation correspond to the case of $T_p = 10eV, T_e = 1eV, T_i = 0.2eV, u_p = 120km/s$ and $B = 50nT$. Conditions of quasineutrality $n_e = n_p + n_i$ and zero net current in the flow (x) direction $u_e = n_p u_p/n_e = \frac{1}{2}u_p$ are imposed on the simulations. The latter condition is a consequence of the one dimensionality and the assumption about the absence of the magnetic field

shear, releasing the condition of zero net current in the analytic dispersion relation it is possible to prove that this condition does not alter the evolution of instability, at least in its linear stage. Results of the simulation are presented in Figures 2 and 3. These results correspond to the case of $\kappa > 1$, smaller κ values have been considered (Quest *et al.*, 1997), but have not been described in this section.

A particle in cell code in which the kinetic evolution of the electron can also be followed has been developed (Quest *et al.*, 2001). In these 1–D particle in cell simulations, Quest *et al.* (2001) demonstrated that significant electron acceleration and heating can occur in the mantle region as a result of the MTSI.

In January 2001, Venus was observed for the first time using an X-ray satellite (Dennerl *et al.*, 2002). Venus is clearly detected as a half-lit crescent, the X-ray emission has been explained as fluorescence scattering of solar X-rays (Dennerl *et al.*, 2002). The emission is observed at discreet energies, mainly the oxygen $K\alpha$ line at 0.53 keV, the carbon $K\alpha$ line at 0.28 keV, and marginally the nitrogen $K\alpha$ line at 0.39 keV. Fluorescent scattering produced by collision between the neutral atmosphere and the energetic electrons cannot be ruled out as another explanation. In fact the lack of solar variability observed in the X-ray spectrum tends to favour the energetic electrons as the source of X-rays.

It is possible to estimate the fluorescence intensity from energetic electron collisions using the following expression for the total X-ray luminosity (Bingham *et al.*, 2008)

$$L_{F\ell} = 10^{-17}\ \pi\ \Lambda\ n_o n_{Te}\ R^2\ \Delta R \frac{1}{\sqrt{\varepsilon_e(eV)}}\ \text{ergs/sec}$$

where the numerical factor Λ for oxygen ($Z = 8$) atoms is 0.1. Using typical planetary and energetic particle values $n_o = 10^5 cm^{-3}, n_{Te} = 10^2 cm^{-3}, \varepsilon_e = 100eV$ and $\Delta R = 10^7 cm$ where n_o is the neutral density at the mantle of width ΔR and distance from planet $R = 10^9 cm$, n_{Te} is the number of accelerated electrons and ε_e their typical energy we calculate the fluorescence luminosity due to energetic electrons as $L_{F\ell} \approx 10^{13}$ erg/sec. The electrons are accelerated by the spectrum of the observed lower-hybrid waves.

Acknowledgments This Paper is dedicated to the memory of Professor Vitali D. Shapiro. This work was partially supported by NASA grant NAG5-11754 as well as the Science and Technology Facilities Council's Centre for Fundamental Physics (CfFP).

References

[Bingham et al.(1991)] Bingham R., Shapiro V. D., Gil'Man M., Tsytovich V. N., de Angelis U., 1991, PhFlB, 3, 1728

[Bingham et al.(2008)] Bingham R., Quest K. B., Shapiro V. D., Kellett B. J., 2008, AnGeo, 26, 1829

[Buneman(1959)] Buneman O., 1959, PhRv, 115, 503

[Crawford T. *et al.*] in Plasma Environments at non Magnetic Planets, ed, by T. Gombosi (Pegamon Press), p.253 (1993).

[Dennerl et al.(2002)] Dennerl K., Burwitz V., Englhauser J., Lisse C., Wolk S., 2002, A&A, 386, 319

[Dobe et al.(1999)] Dobe Z., Quest K. B., Shapiro V. D., Szego K., Huba J. D., 1999, PhRvL, 83, 260

[Grard et al.(1989)] Grard R., Pedersen A., Klimov S., Savin S., Skalskii A., 1989, Natur, 341, 607

[Hsia et al.(1979)] Hsia J. B., Chiu S. M., Hsia M. F., Chou R. L., Wu C. S., 1979, PhFl, 22, 1737

[Huba(1993)] Huba J. D., 1993, GeoRL, 20, 1751

[McBride & Ott(1972)] McBride J. B., Ott E., 1972, PhLA, 39, 363

[McBride et al.(1972)] McBride J. B., Ott E., Boris J. P., Orens J. H., 1972, PhFl, 15, 2367

[Quest et al.(1997)] Quest K. B., Shapiro V. D., Szegö K., Dobe Z., 1997, GeoRL, 24, 301

[Quest, Ucer, & Shapiro(2001)] Quest K. B., Ucer D., Shapiro V. D., 2001, APS..DPPB, 1022P

[Rosenbauer et al.(1989)] Rosenbauer H., Shutte N., Galeev A., Gringauz K., Apathy I., 1989, Natur, 341, 612

[Sagdeev et al.(1990)] Sagdeev R. Z., Shapiro V. D., Shevchenko V. I., Zacharov A., Kiraly P., Szego K., Nagy A. F., Grard R. J. L., 1990, GeoRL, 17, 893

[Scarf et al.(1980)] Scarf F. L., Taylor W. W. L., Russell C. T., Elphic R. C., 1980, JGR, 85, 7599

[Shapiro et al.(1995a)] Shapiro V. D., Szegö K., Ride S. K., Nagy A. F., Shevchenko V. I., 1995a, JGR, 100, 21289

[Shutte et al.(1989)] Shutte N. M., Diachkov A. V., Kiraly P., Cravens T. E., Gombosi T. I., 1989, Natur, 341, 614

[Strangeway & Russell(1996)] Strangeway R. J., Russell C. T., 1996, JGR, 101, 17313

[Szego et al.(1991)] Szego K., Shapiro V. S., Shevchenko V. I., Sagdeev R. Z., Kasprzak W. T., Nagy A. F., 1991, GeoRL, 18, 2305

[Szegő et al.(1997)] Szegő K., Dóbé Z., Knudsen W. C., Nagy A. F., Shapiro V. D., 1997, JGR, 102, 2175

[Taylor et al.(1980)] Taylor H. A., Brinton H. C., Bauer S. J., Hartle R. E., Cloutier P. A., Daniell R. E., 1980, JGR, 85, 7765

1 Figure captions

FIG. 1: Relationship between the maximum growth rate and wave frequency for the different κ values ($\kappa = \frac{k_{||}}{k}\sqrt{\frac{m_p}{m_e}}$), solid line analytical calculations, triangles correspond to simulation results of the dispersion relation (89) for the modified two stream instability.

FIG. 2: Phase space plots of protons and oxygen ions at saturation of the linear instability (left hand plots) and in the fully developed turbulent phase (right hand plots).

FIG. 3: Evolution in time for different k of the bulk momentum for (a) solar wind protons and (b) oxygen ions. Both are normalised to the initial proton bulk momentum.

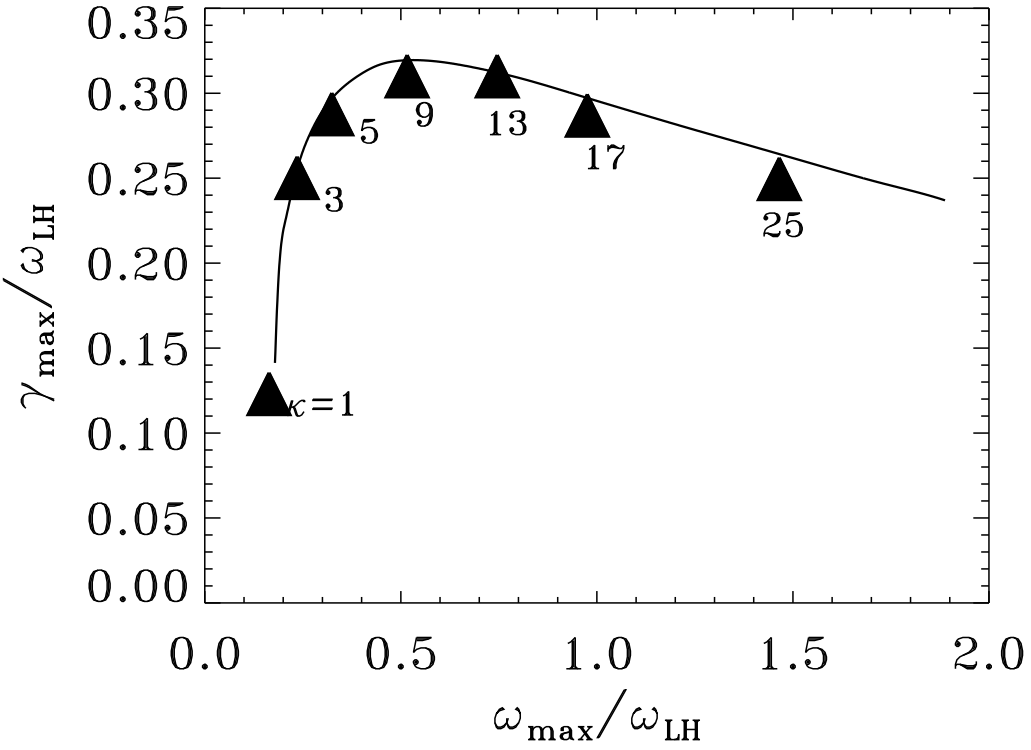
0.35
0.30
0.25
0.20
0.15
0.10
0.05
0.00
0.0
0.5
1.0
1.5
2.0
γ_{max}/ω_{LH}
ω_{max}/ω_{LH}
κ=1
3
5
9
13
17
25

Figure 1:

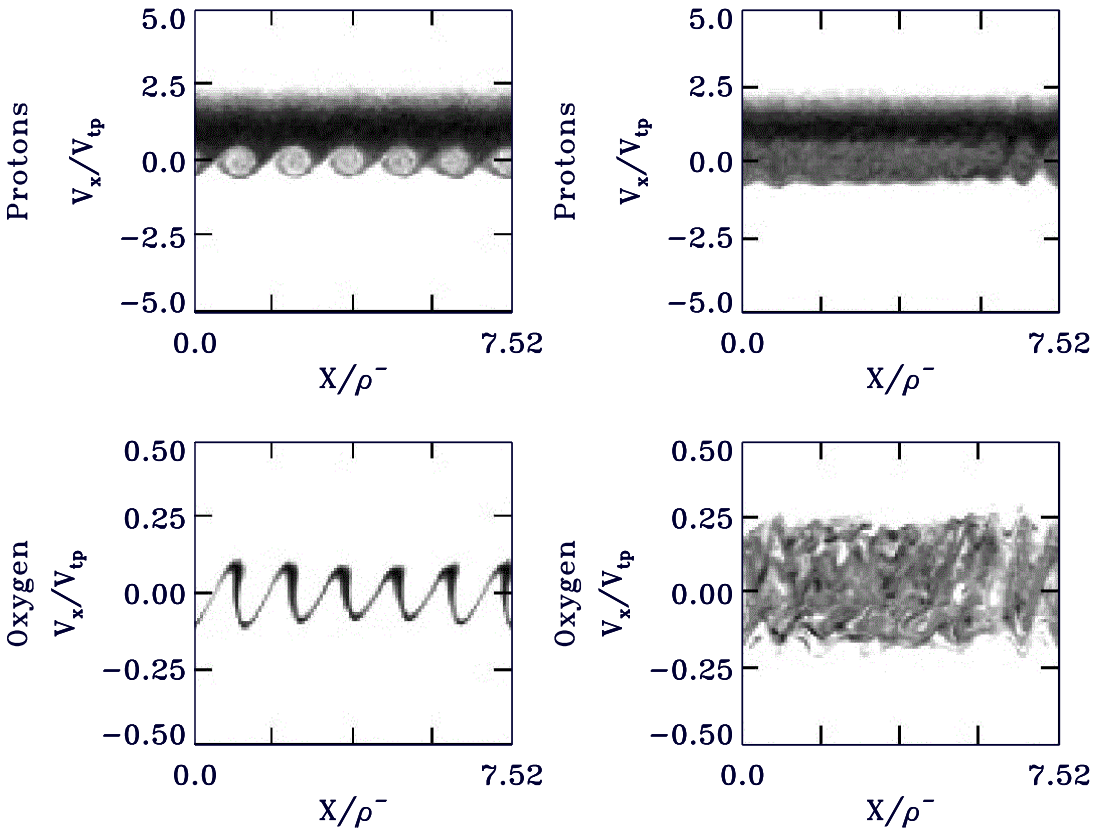
Protons
V_x/V_{tp}
5.0
2.5
0.0
−2.5
−5.0
0.0
7.52
X/ρ^-
Protons
V_x/V_{tp}
5.0
2.5
0.0
−2.5
−5.0
0.0
7.52
X/ρ^-
Oxygen
V_x/V_{tp}
0.50
0.25
0.00
−0.25
−0.50
0.0
7.52
X/ρ^-
Oxygen
V_x/V_{tp}
0.50
0.25
0.00
−0.25
−0.50
0.0
7.52
X/ρ^-

Figure 2:

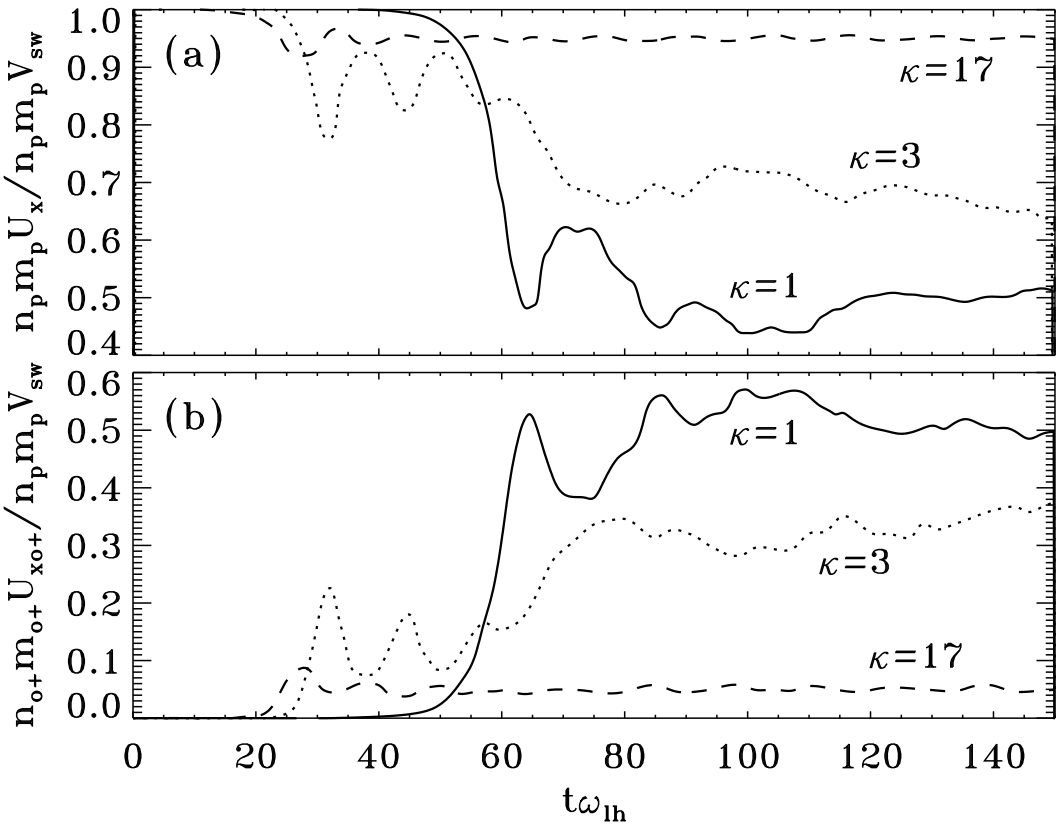

Figure 3: